Molecular Processes Leading to "Necking" in Extensional Flow of Polymer Solutions Using Microfluidics and Single DNA Imaging

Sachdev, Shaurya; Muralidharan, Aswin; Boukany, Pouyan E.

DOI
10.1021/acs.macromol.6b01755

Publication date
2016

Document Version
Final published version

Published in
Macromolecules

Macromolecules

Article

pubs.acs.org/Macromolecules

Molecular Processes Leading to "Necking" in Extensional Flow of Polymer Solutions: Using Microfluidics and Single DNA Imaging

Shaurya Sachdev, Aswin Muralidharan, and Pouyan E. Boukany*

Department of Chemical Engineering, Delft University of Technology, 2629 HZ, Delft, The Netherlands

Supporting Information

ABSTRACT: We study the necking and pinch-off dynamics of liquid droplets that contain a semidilute polymer solution of polyacrylamide close to overlap concentration by combining microfluidics and single DNA observation. Polymeric droplets are stretched by passing them through the stagnation point of a T-shaped microfluidic junction. In contrast with the sudden breakup of Newtonian droplets, a stable neck is formed between the separating ends of the droplet which delays the breakup process. Initially, polymeric filaments experience exponential thinning by forming a stable neck with extensional flow within the filament. Later, thin polymeric filaments develop a structure resembling a series of beads-on-a-string along their length and finally rupture during the final stages of the thinning process. To unravel the molecular picture behind these phenomena, we integrate a T-shaped microfluidic device with advanced fluorescence microscopy to visualize stained DNA molecules at the stagnation point within the necking region. We find that the individual polymer molecules suddenly stretch from their coiled conformation at the onset of necking. The extensional flow inside the neck is strong enough to deform and stretch polymer chains; however, the distribution of polymer conformations is broad, and it remains stationary in time during necking. Furthermore, we study the dynamics of single molecules during formation of beads-on-a-string structure. We observe that polymer chains gradually recoil inside beads while polymer chains between beads remain stretched to keep the connection between beads. The present work effectively extends single molecule experiments to free surface flows, which provides a unique opportunity for molecular-scale observation within the polymeric filament during necking and rupture.

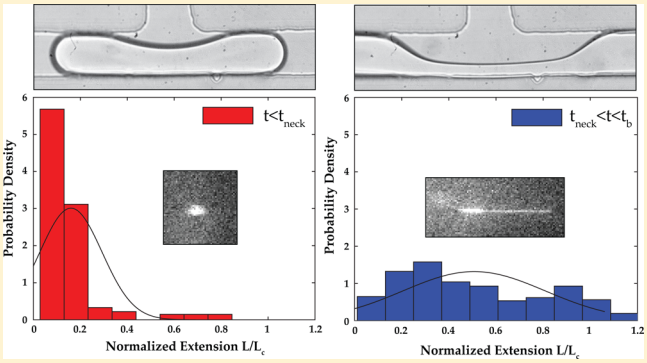

INTRODUCTION

The extensional flow and breakup of liquid droplets are strongly affected by the presence of a very small amounts of long macromolecules. For instance, during jet breakup, or when a drop of pure water falls from a faucet or a nozzle, it suddenly necks down under the capillary forces and pinches off into smaller droplets.[1] If a small amount of polyacrylamide (PAA) or poly(ethylene oxide) (PEO) is added to water, this sudden rupture (or pinching) is delayed and instead a stable "neck" is formed that thins down slowly over time.[2−5] The process of neck formation is a ubiquitous feature in all extensional flows of polymeric fluids and happens at all length scales.[6] Therefore, characterizing the extensional rheology of polymer solutions not only is of fundamental importance for studying the stable neck formation but also is important for a large number of commercially relevant processes that are influenced by it. A few examples are fiber spinning, nanowire array formation, roll-coating of adhesive, ink jet printing, spray formation, porous media flows, and turbulent drag reduction.[7−9]

Extensional flows of free surface polymer solutions were traditionally investigated by filament stretching extensional rheometer (FiSER)[10] or capillary breakup extensional rheometer (CaBER)[11] devices. FiSER devices can produce homogeneous extensional flows by sandwiching a polymer solution between two circular end-plates and moving them apart with the constant imposed extension rate, $\dot{\varepsilon}$.[12] In CaBER devices, a polymeric fluid is also placed between two circular end-plates (of radius R) and stretched with an exponential profile to form a liquid bridge with the final stretch length $L \approx 3.6R$. The stretch is then stopped, and the developed liquid bridge thins under capillary forces, resulting in the generation of an extensional flow within the cylindrical polymeric filament.[13] The shape of the polymeric filament leads to higher capillary pressure inside the filament than in the end regions of the filament which squeezes the polymeric fluid toward the upper and lower end-plates. This creates a self-thinning of the thread, and the evolution of the thread diameter is observed while the thread thins and finally breaks.[6,13] For Newtonian solutions, the extensional viscosity is 3 times the shear viscosity. However, for polymer solutions, the transient extensional viscosity can be orders of magnitude higher than the shear viscosity at high $\dot{\varepsilon}$.[14] Recently, Liu et al.[15] investigated the

Received: August 11, 2016
Revised: November 18, 2016
Published: December 15, 2016

DOI: 10.1021/acs.macromol.6b01755
Macromolecules 2016, 49, 9578−9585

origin of strain hardening during the startup uniaxial extension of polymer melts and suggested that this phenomenon may originate from the difference in the kinematics between shear and extension. In addition, they found that the geometric condensation occurs in startup uniaxial extension and can produce noticeable strain hardening.[15] When the flow becomes strong enough (at extension rates larger than the characteristic relaxation time of the polymeric fluid, $\dot{\varepsilon}\tau \geq 0.5$),[16] the effective viscosity of the polymeric fluid can be increased dramatically due to polymeric chain stretching.[6] This high transient extensional viscosity is able to resist the extensional deformation and leads to the formation of a stable neck during extensional flow and capillary thinning.[6] Elastic forces developed within the flow of the polymer solutions are able to resist the capillary forces during jet breakup, giving rise to the high extensional viscosity.[6,12,17] From a molecular point of view, these elastic forces originate due to the orientation and stretching of polymer molecules in the direction of the flow or the extensional deformation.[6,12,17,18] Thus, in order to better characterize the extensional rheology of polymer solutions, it is essential to elucidate the molecular picture behind extensional deformation and stable neck formation.

Using microfluidics integrated with a fluorescence microscope has allowed polymer scientists to study the conformation of fluorescently stained DNA in controlled flow conditions and examine polymer theories directly against experimental observations at the single-chain level.[8,19−26] In 1974, de Gennes predicted that a sharp coil−stretch transition occurs in a homogeneous extensional flow of dilute polymer solution, if the extension rate exceeds a critical value of the Weissenberg number ($Wi = \dot{\varepsilon}\tau$).[16] Experimentally, Chu's group at Stanford used a microfluidic cross-slot device to trap single DNA molecules at the stagnation point of an extensional flow and visualized the evolution of individual DNA molecules during the extensional flow to validate this theoretical prediction.[8,27] They found that most of the DNA molecules are highly aligned and stretched at high $Wi \approx 3$, after sufficient residence time in the extensional flow.[27] So far, the coil−stretch transition has been observed in single phase extensional flow of linear and circular DNA molecules beyond a critical $\dot{\varepsilon}$ (when $Wi \geq 1$) in the microfluidic cross-slot geometry.[20,22,23] However, to address neck formation, and breakup of polymeric fluids, one needs to perform single DNA molecule experiments in free surface flows of polymer solutions inside a microfluidic device.

While considerable effort has been dedicated to characterize the extensional rheology of polymer solutions using microfluidics,[28] microfluidics has also been used to study the jet breakup of polymer solutions leading to a stable neck.[29−36] Thus, microfluidics, owing to the length scales involved, provides a suitable platform for measuring the bulk flow behavior of the stable neck and simultaneously observing the individual molecules inside it.[37] Recently, co-flowing microfluidic devices have been used to study the polymeric jet breakup and stable neck formation and observe the conformation of DNA molecules inside them.[35,36] An inherent disadvantage with these geometries is the lack of a stagnation point. Therefore, either it is not possible to make molecular observations in the stable neck due to high velocities and motion blur,[35] or the observations have to be corrected for the motion blur.[36] To overcome this limitation, we propose to employ a microfluidic T-junction to visualize single DNA molecules inside polymeric filaments by generating polymeric droplets and passing them through the stagnation point at a T-junction.

In this work, we integrate a T-junction microfluidic geometry with DNA imaging to capture the molecular picture behind the neck formation in extensional flow of aqueous polymer solutions. In particular, we use semidilute solution of long-chain PAA molecules seeded with fluorescently stained DNA molecules (T4-DNA with similar contour length) to link between the microscopic properties of the solution and the thinning dynamics of polymeric filaments during extensional flow. The presence of a stagnation point in microfluidic T-junctions allows for the observation of individual DNA molecules in the stable neck. Since DNA molecules are seeded or dissolved in the polymer solution, they act as markers or probes for the polymers in the solution and hence reflect the conformation of polymer molecules. With this argument, we find that the initially coiled polymer molecules elongate suddenly at the onset of the neck formation, giving rise to a high extensional viscosity in polymer solutions. We find nearly full extension of polymer molecules in the bulk of the neck; however, they display a broad distribution of the molecular extensions due to molecular individualism. Furthermore, beads-on-a-string morphology observed at the very last stage of the polymeric droplet breakup is also explored using single molecule observations. As such, we demonstrate a simple and effective microfluidic tool which has the capability to characterize the extensional flow of polymer solutions at both microscopic and macroscopic level.

EXPERIMENTAL SECTION

To analyze the filament thinning and droplet deformation, a T-shaped microfluidic chip is fabricated from polydimethylsiloxane (PDMS) using the standard soft lithography technique.[38−39] Microfluidic channels are sealed with a glass slide coated with a thin layer of PDMS after treating both top and bottom surfaces with an oxygen plasma. The assembled microfluidics is baked in the oven for 12 h at 68 °C to complete the curing process. To ensure that the walls are more hydrophobic, the baked chips are also exposed to trichloro-(1*H*,1*H*,2*H*,2*H*-perfluorooctyl)silane inside a desiccator for at least 12 h. A schematic picture of the entire geometry is shown Figure 1. Silicone oil (50 cst, Sigma-Aldrich) constitutes the continuous phase and enters the microfluidic geometry through channel i. The polymer solution constitutes the dispersed phase and enters the microfluidic geometry through channel ii. At the intersection of channels i and ii, the stable polymeric droplet is formed (without using a surfactant). An

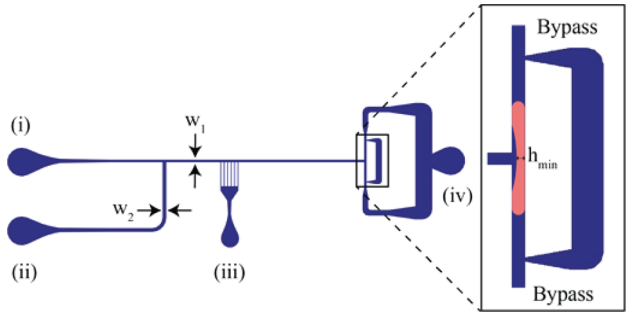

Figure 1. Microfluidic T-junction geometry used to study polymeric droplet breakup. (i) Inlet channel for the continuous phase, 50 cst silicone oil. (ii) Inlet channel for the dispersed phase, aqueous polymer solution. (iii) Additional inlet for the continuous phase to adjust the spacing between the droplets. (iv) Outlet. The width of the main channel, W_1, is 100 μm, and W_2 is 150 μm. The height of the microfluidic chip (H) is 100 μm.

DOI: 10.1021/acs.macromol.6b01755
Macromolecules 2016, 49, 9578−9585

additional continuous phase inlet for silicone oil is provided (channel iii). This is used to adjust the spacing between the droplets. This droplet then travels downstream at constant velocity (≈ 3300 μm/s) and reaches the T-junction where it is pulled into the two arms. The droplet then starts to thin due to a buildup of pressure at the upstream of the two arms and low pressure at the downstream of the two arms (see zoomed image of the T-junction). Two bypass junctions are provided to equalize the pressure downstream of the two arms. The continuous phase inlet flow rate is 0.2 μL/min, and the dispersed phase inlet flow rate is 0.1 μL/min. The additional continuous phase inlet flow rate is 1 μL/min. The combination of these flow rates gives the best droplet production stability.

The flow images, or droplet thinning dynamics, are captured in bright-field using a Zeiss Axiovert 100M microscope connected with a high-speed camera (Phantom V9.1, 1600 × 1200 pixels). The bright-field images are obtained at 20× magnification and 1000 frame per seconds (fps) with an exposure time of 150 μs. For the DNA imaging, a tiny amount of T4-DNA as tracer molecules is added to the polymer solution. First, 10 μL of T4-DNA solution (used as received from Nippon Gene Co. Ltd. at a concentration of 440 μg/mL in 10 mM Tris (pH = 8.0) and 1 mM EDTA) is stained using the YOYO-1 dye (Molecular Probes Inc.) at a base-pair:dye ratio of 5:1. The solution is then diluted to 4.4 μg/mL in Milli-Q. Finally, ≈20 μL of this solution is added to 5 mL of the polymer solution, thus making the final concentration of tracer T4-DNA as ≈0.01 ppm. We find that the presence of DNA tracers does not affect the thinning and breakup dynamics of our solutions (see Figure S1 in the Supporting Information). The reason for choosing T4-DNA is that it has a similar contour length (≈56 μm) as PAA (≈53 μm) which allows for a direct correlation between molecular conformations of T4-DNA and PAA. DNA imaging is carried out on a fluorescence microscope (Zeiss AxioObserver-Z1) coupled with an EMCCD camera (ANDOR ixon3). A 63× objective lens with water immersion is used for an optimal magnification with a numerical aperture (NA) of 1.0 and working distance of 2.1 mm. The field of view is 110 μm × 110 μm with a resolution of 512 × 512 or 128 × 128 pixels using frame rates varying between 33 and 125 fps, which is fast enough to capture the DNA dynamics without motion blur.

We focus on the extensional flow behavior of PAA (Polysciences Inc., average molecular weight M_w = 18 × 10^6 g/mol) at a concentration of 200 μg/mL in two different solvents. Radius of gyration R_g of this polymer molecule in water is around 0.33 μm with a contour length (L_c) of 53 μm.[31,36,40] The overlap concentration of this polymer in water (C^*) is also around 200 μg/mL calculated as $C^* = \frac{3M_w}{4\pi N_A (R_g)^3}$, where M_w is the molar mass of the chain, N_A is the Avogadro number, and R_g is the radius of gyration of polymer in a dilute solution.[41] Note that PAA is a charged polymer, meaning that the polymer coils could be extended beyond the random coil configuration in pure water, and the above expression is probably an overestimate of the coil overlap concentration.[42] To prepare polymer solutions as the dispersed phase, we dissolve the PAA polymer (used as received from Polymer sciences Inc.) at a concentration of 200 μg/mL ($C \approx C^*$) in two different solvents including pure water (Milli-Q) or glycerol−Milli-Q (25%−75% in volume). We also tested concentrations of PAA solutions less than 200 μg/mL. PAA solutions made with 200 μg/mL provided a stable neck that persisted for a sufficient amount of time to allow for molecular observations (see Figure S1 in the Supporting Information for more details). We note that for samples at low polymer concentrations (C < 100 μg/mL) droplets rupture like Newtonian droplets without exhibiting a stable neck formation due to their lower viscoelasticities.

To characterize the viscoelastic properties of polymer solutions, rheological measurements are performed. All rheological measurements are carried out on a TA AR2000 rheometer with Couette configuration (with a cup of 30 mm and a bob of 28 mm) at room temperature. To check reproducibility of our measurements, all rheological and thinning experiments are carried out at least in triplicate. The viscosity of the Newtonian solvent (η_{sol}) is 1 and 2.5 mPa·s for only Milli-Q and 25% glycerol−Milli-Q (v/v), respectively. The two polymer solutions, PAA in only Milli-Q and PAA in 25% glycerol−Milli-Q (v/v), show strong shear thinning with zero shear viscosity of 6 and 3 Pa·s, respectively (see Figure 2). The variation of

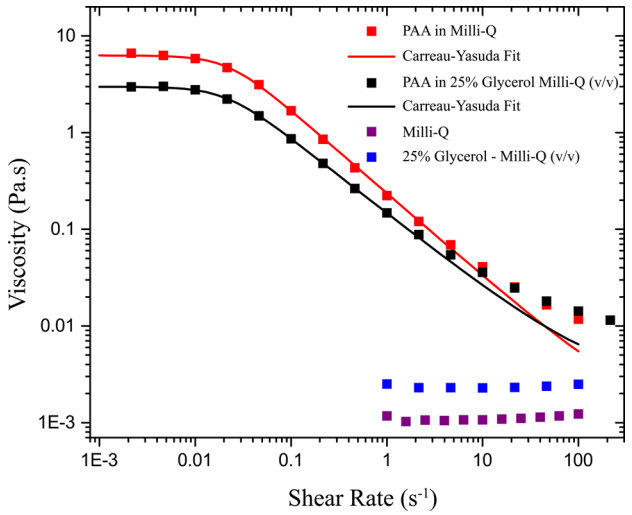

Figure 2. Steady shear viscosity curves for Newtonian solvents (Milli-Q and 25% glycerol-Milli-Q (v/v)) and rheology of the PAA solutions (C = 200 μg/mL) used in this study. All shear experiments are carried out at room temperature.

shear viscosity (η) with imposed shear rate can be fitted with the Carreau−Yasuda model: $\frac{\eta - \eta_\infty}{\eta_0 - \eta_\infty} = [1 + (\tau\dot{\gamma})^a]^{(n-1)/a}$. Here η is the measured shear viscosity, η_0 is the zero shear viscosity, η_∞ is the shear viscosity at infinite shear rate (close to solvent viscosity), $\dot{\gamma}$ is the imposed shear rate, τ is a characteristic relaxation time (close to the reciprocal shear rate at which shear thinning occurs during shear), n is the power-law exponent, and a represents the width of the transition region from the zero shear viscosity η_0 to the shear thinning or the power-law region. The fittings of the Carreau−Yasuda model to the experimental measurements of the steady shear rheology are displayed in Figure 2. These solutions are shear thinning fluids with power law index around $n \approx 0.13$ and $n \approx 0.25$ for water and glycerol−water mixtures, respectively. It is well established that PAA solutions exhibit strong shear thinning in the nonionic solvents (in the absence of salt).[42] The relaxation time from the Carreau−Yasuda model gives $\tau_{CY} \approx 45$ s and $\tau_{CY} \approx 53$ s for water and glycerol−water mixtures, respectively. Such high relaxation times were reported for PAA solutions, which could be attribute to the nonionic solvent and polydispersity of PAA.[42,43] Typically, the persistence length of PAA in high ionic solvent is 2.7 ± 0.9 nm.[40,44] In the absence of salt, the persistence length of PAA can be of ≈O(100 nm).[40] This can probably increase the relaxation time of the polymer system since it has been shown previously that the onset of shear thinning regime in steady shear flows happens at lower shear rates for hydrolyzed polyacrylamides (HPAM) in nonionic solvents as opposed to ionic solvents.[45,46] We also investigate the flow response of PAA solutions (200 μg/mL) in the presence of salt (10 mM NaCl), and the steady shear rheology of PAA solutions with addition of salt (10 mM NaCl) is shown in Figure S3.

Zimm relaxation time of polymer solutions τ_Z is approximately 0.01 and 0.03 s for pure Milli-Q and 25% glycerol−Milli-Q (v/v) solutions, respectively, estimated as $\tau_Z = \frac{\eta_{sol}(R_g)^3}{k_B T}$, where η_{sol} is the solvent viscosity, k_B is the Boltzmann's constant, and T is the absolute temperature of the solution.[47] The interfacial surface tensions of solutions (with employed silicone oil) determined by the pendant drop technique are $\gamma \approx 35$ mN/m and $\gamma \approx 12$ mN/m for pure Milli-Q and a 25% glycerol−Milli-Q (v/v) solution, respectively (see Figure S2). All measurements are carried out at room temperature. For these set of conditions, the Reynold's number based on the zero shear

DOI: 10.1021/acs.macromol.6b01755
Macromolecules 2016, 49, 9578−9585

viscosity is $Re \approx O(10^{-4}-10^{-3})$ and the Capillary number is $Ca \approx O(10^{-3}-10^{-2})$. The Reynolds number ($Re$) is defined as $Re = \rho U l/\eta$, where ρ is the fluid density, U is the velocity of the flow, η is the fluid viscosity, and $l = 2WH/(W + H)$ is the characteristic length ($l \approx W$, when $W \approx H$); here $W = 100$ μm and $H = 100$ μm are the characteristic width and depth of the microchannel, respectively.[37] The Ca is defined as $Ca = \eta U/\gamma$, where γ is the interfacial tension between the continuous and dispersed phases.

RESULTS AND DISCUSSION

First, we monitor the change in the thickness of the filament that holds the droplet as a function of time during the droplet stretching or pinch-off at the T-junction. Representative snapshots of the stretched liquid droplets at the stagnation point and the necked region undergoing thinning in Newtonian and polymer solutions are shown in Figure 3a–d. In the first case, we investigate the breakup of a Newtonian droplet for comparison and reference purposes (see Figure 3b). The Newtonian system considered here is an aqueous glycerol solution (25% glycerol–Milli-Q (v/v)). Figure 3b shows the breakup as a function of t/t_b, where t_b is the breakup time of the droplet ($t_b \approx 0.05$ s). $t = 0$ is taken as the instant when the droplet completely occupies the two arms of the T-junction and the width of the droplet is equal to the width of the channel of the T-junction. There is a buildup of pressure at the upstream end of the droplet because of the flowing outer phase (50 cst silicone oil). Since the droplet completely occupies the two arms of the T-junction, the pressure downstream in the two arms of the droplets is reduced. Thus, a pressure drop is created, with high pressure at the center of the droplet and low pressure at the two ends of the T-junction. This pressure drop squeezes the droplet until it eventually breaks. As can be seen from Figure 3b, the Newtonian droplet pinches off suddenly without exhibiting a stable neck formation at $t/t_b \approx 0.9$ (see Movie S1).

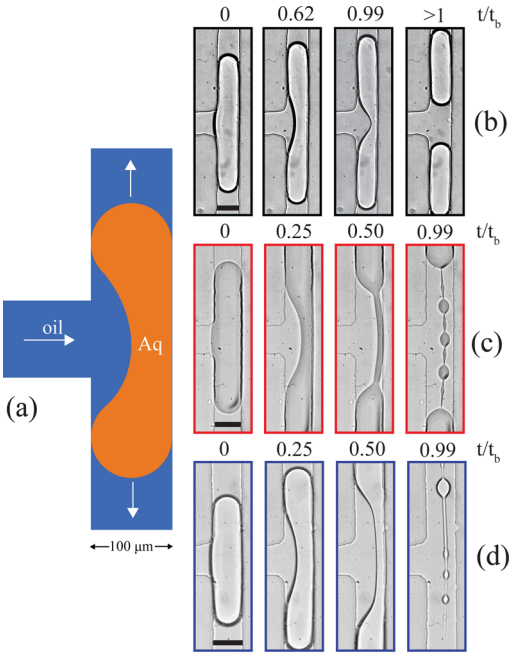

Figure 3. (a) Microfluidic T-junction geometry used to stretch liquid droplets. Sequences of images comparing the breakup of Newtonian and polymeric droplets. (b) Breakup of Newtonian (25% glycerol–Milli-Q (v/v)) droplets (with $t_b \approx 0.05$ s). Stretching and thinning of PAA fluids in (c) Milli-Q (with $t_b \approx 0.19$ s) and (d) 25% glycerol–Milli-Q (v/v) (with $t_b \approx 0.47$ s) at the T-junction. The scale bar is 100 μm.

The breakup of polymeric droplets at the microfluidic T-junction is shown in Figure 3c,d. The polymeric droplet initially starts to thin by a similar mechanism as the Newtonian droplet. However, these droplets do not pinch off suddenly, and the breakup is delayed. Figure 3c,d reveals that the droplet behaves differently from its Newtonian counterpart (at $t/t_b \approx 0.5$). A stable neck is formed between the breaking ends which significantly delays the breakup (see Movie S2 and Movie S3). While the formation of a neck could be observed in both polymeric systems, we focused on PAA dissolved in 25% glycerol–Milli-Q (v/v) solution, as the necking process is slower and easier to analyze for DNA imaging. In both polymeric solutions, beads-on-a-string structure has been observed at the late stage of the pinch-off process ($t/t_b \approx 1$).

To quantify the breakup event, the breakup dynamics are measured for both the Newtonian droplets and the polymeric droplets (see Figure 4a). The breakup dynamics is measured by tracking the interface of the thinning droplet. The interface is tracked where the thickness of the droplet is minimal which occurs at the middle of the T-junction. This minimum thickness is referred to as h_{min}. From the breakup dynamics of the Newtonian droplet it is clear that the droplet snaps off instantly when the minimum thickness reaches a value around 70 μm. This sudden snap-off behavior is common for Newtonian systems and has also been observed previously and is referred to as the singular behavior or finite time singularity.[5,48] For polymeric droplets, it can be seen that the breakup dynamics are exactly similar to the Newtonian droplet for early times ($t < 0.05$ s). However, after $t \approx 0.05$ s, the breakup dynamics start to diverge. The polymeric droplet forms a stable neck that thins down slowly with time.

The necking part (from $t \approx 0.05$ s to beads-on-a-string regime) of the thinning dynamics of the polymeric droplet is subjected to an exponential fit of the form $h_{min} \propto \exp\left(-\frac{1}{2}\dot{\epsilon}t\right)$, where $\dot{\epsilon}$ is the extensional strain rate. From Figure 4b, it can be seen that the exponential fit well approximates the thinning dynamics of the droplet in the neck with $\dot{\epsilon} \approx 28$ and 10 s^{-1} for PAA solution in Milli-Q and 25% glycerol–Milli-Q (v/v), respectively. Such an exponential decay of h_{min} with time is characteristic of a pure extensional flow and has been previously observed in various configurations producing an extensional flow[5,12,17,49] and has also been predicted by theory.[18] This suggests that the flow inside the stable neck observed in microfluidic T-junction is extensional. By assuming that $Wi = \dot{\epsilon}\tau_{eff} = 2/3$, we can estimate the effective relaxation of $\tau_{eff} \approx 0.02$ and 0.06 s corresponding to the PPA solution in Milli-Q and aqueous glycerol (25% glycerol–Milli-Q (v/v)), respectively.[17] Our estimated τ_{eff} is of the same order of magnitude as the estimated τ_Z. Furthermore, the accumulated Hencky strain can be calculated as $\varepsilon = -2\ln\left(\frac{h_{min}(t)}{h_0}\right)$, where h_0 is the initial thickness of droplet (at $t = 0$).[17] Figure 4c displays that beads-on-a-string structure has been formed at $\varepsilon \approx 4$ in both PAA solutions. Figure 4d displays the estimated transient extensional viscosity calculated as $\eta_e = \frac{2\gamma}{\dot{\epsilon}h_{min}(t)}$ for both solutions.[17] It is well-established that transient η_e can be orders of magnitude larger than shear viscosity, and it is strongly dependent on time (or ε), as shown in Figure 4d. In addition, we investigate the

DOI: 10.1021/acs.macromol.6b01755
Macromolecules 2016, 49, 9578–9585

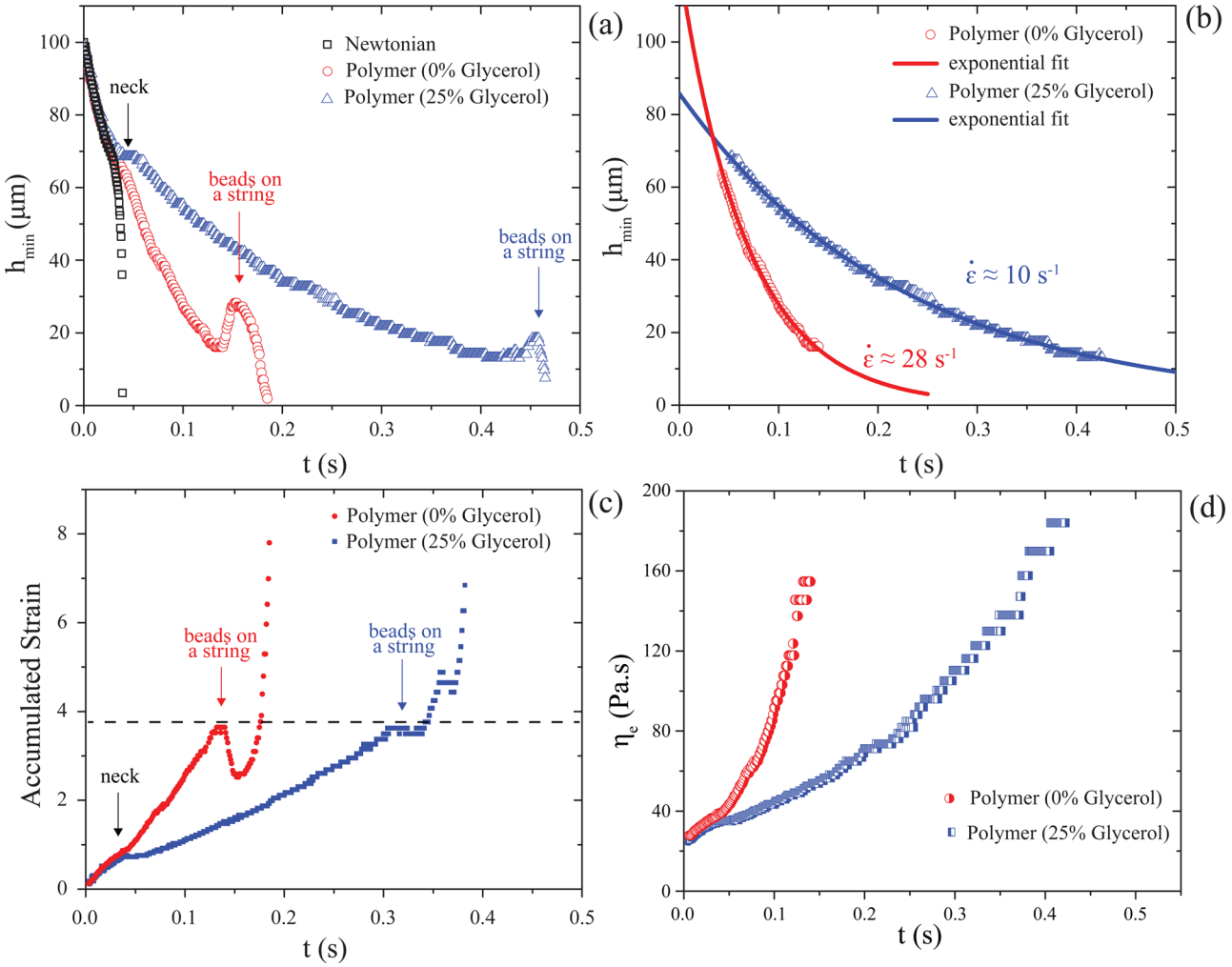

Figure 4. (a) Breakup dynamics calculated by measuring the h_{min} as a function of time for both Newtonian and polymeric droplets (approximately 5−10 droplets are analyzed for each set of operating conditions). (b) Strain rate ($\dot{\varepsilon}$) is estimated by exponential fitting of the breakup dynamics during necking. $\dot{\varepsilon} = 27.3 \pm 3.3\ s^{-1}$ and $\dot{\varepsilon} = 9.8 \pm 1.1\ s^{-1}$ for PAA solution in Milli-Q and 25% glycerol−Milli-Q (v/v), respectively. (c) Accumulated Hencky strain is calculated as $\varepsilon = -2 \ln\left(\frac{h_{min}(t)}{h_0}\right)$ for both PAA solutions.[17] (d) Transient extensional viscosity of PAA solutions against time.

thinning dynamics of PAA solution (with 10 mM NaCl). With this salt concentration, we expect that polymer chains are fully neutralized and electrostatic effects are minimized.[50] Qualitatively, similar thinning behavior has been observed in PAA solution with 10 mM NaCl (see Figure S4).

Having validated the microfluidic T-junction for producing a stable neck with an extensional flow inside, we continued investigating the conformations of the polymer molecules by direct visualization inside this neck. Since it is currently difficult to directly stain the polymer (PAA) molecules,[36] stained T4-DNA molecules of comparable contour length are added to the solution. We assumed that the individual dynamics of the T4-DNA molecules would be representative of the polymer molecules producing the neck.[8,36,51−54] The dynamics of individual DNA molecules at different stages of thinning is shown in Figure 5b. During the initial stages of the breakup, the thinning dynamics of the polymer and the Newtonian droplet are the same, which implies that the role of the polymer molecules is absent during this stage. The macromolecules remain coiled and are not influencing the breakup dynamics (see Figure 5a,b). However, at the onset of necking, the macromolecules elongate suddenly, as shown by the last two snapshots of Figure 5b. The extensions of the DNA molecules are measured both before and during stable neck formation (see Figure 5c,d) as the probability density of normalized lengths. Figure 5c confirms that before necking, majority of the DNA molecules are in their equilibrium coiled conformation. In contrast, during the neck formation, the majority of these polymer molecules are stretched due to the extensional flow inside the stable neck. The *Wi* number can be calculated as $Wi = \dot{\varepsilon}\tau_{CY} \approx 530$, where $\dot{\varepsilon} \approx 10\ s^{-1}$ and $\tau_{CY} \approx 53$ s from shear rheology. The strain accumulated over the entire process of necking is $\varepsilon \approx 4$ (as shown in Figure 4c) before the neck transforms into a beads-on-a-string morphology. Such a high *Wi* number and accumulated strain are enough to stretch the polymer molecules from their equilibrium coiled conformation. Despite such high *Wi*, the level of stretch or the molecular extension of individual DNA molecules is rather heterogeneous with a broad distribution as shown in Figure 5d. The level of this heterogeneity could possibly be explained by molecular individualism and different preshear conditions and has been previously observed as well.[25,27,35] Apart from this, a few DNA molecules are prestretched beyond their equilibrium coiled conformation before the formation of stable neck (see Figure

DOI: 10.1021/acs.macromol.6b01755
Macromolecules 2016, 49, 9578−9585

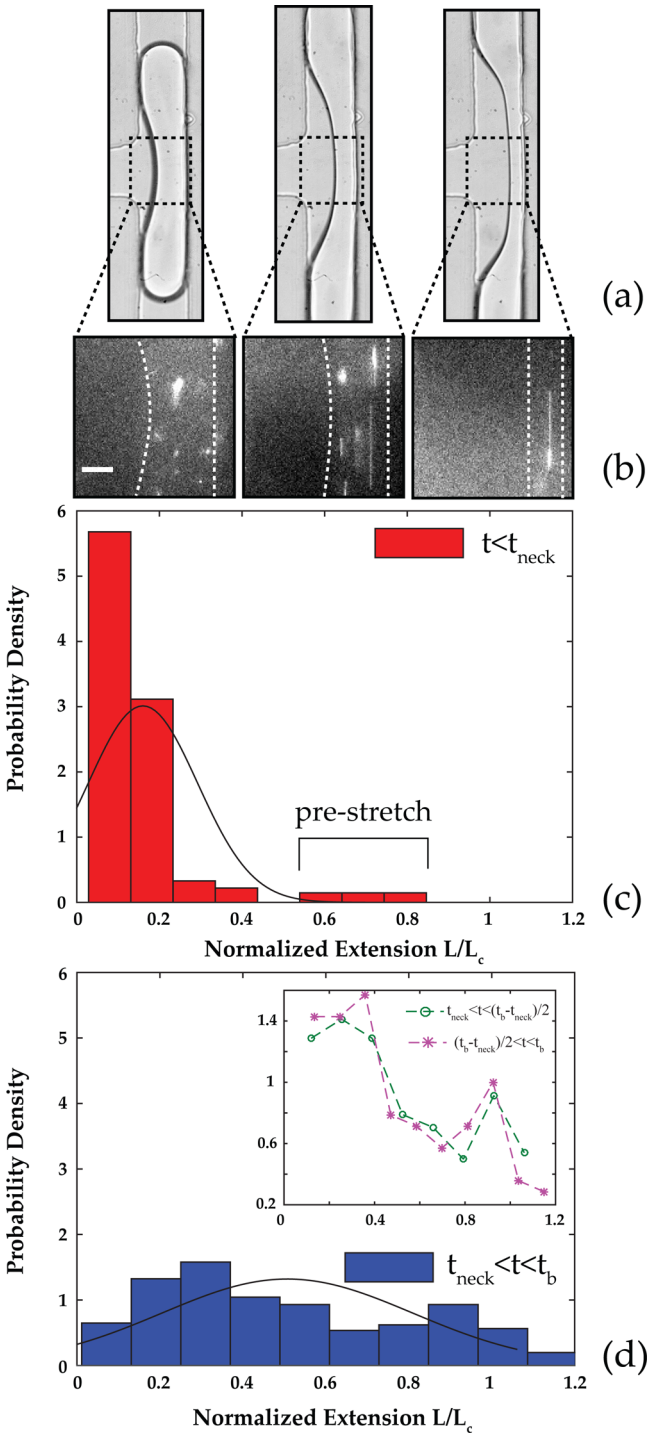

Figure 5. (a, b) Snapshots showing how DNA molecules behave during the neck formation (the snapshots are separated by an interval of 15 ms). Scale bar is 35 μm. Probability density of the extension of the DNA molecules is shown in (c) before and (d) after the neck formation. The probability density functions (PDF) are constructed using 600 measurements. The inset shows that PDF is almost insensitive to the time during necking.

5c). The inset of Figure 5d confirms that the variation of the extensions during necking is insensitive to the necking time, and the probability distribution is almost the same when the data are separated into two groups. A similar distribution has been observed in PAA solution in 50% glycerol (see Figure S6) and also for PAA solution (200 μg/mL dissolved in 25% glycerol−Milli-Q (v/v)) with 10 mM NaCl (see Figure S5). Thus, it can be concluded that the electrostatic effects are negligible or at least small compared to the effect of extension in our PAA solutions (in the range we studied). The stretching and deformation of macromolecules contribute additional tensile elastic stresses, which stabilize the neck formation by opposing capillary stress during thinning.

During the last stages of the breakup, the stable neck transforms into beads-on-a-string morphology (see Figure 6a).

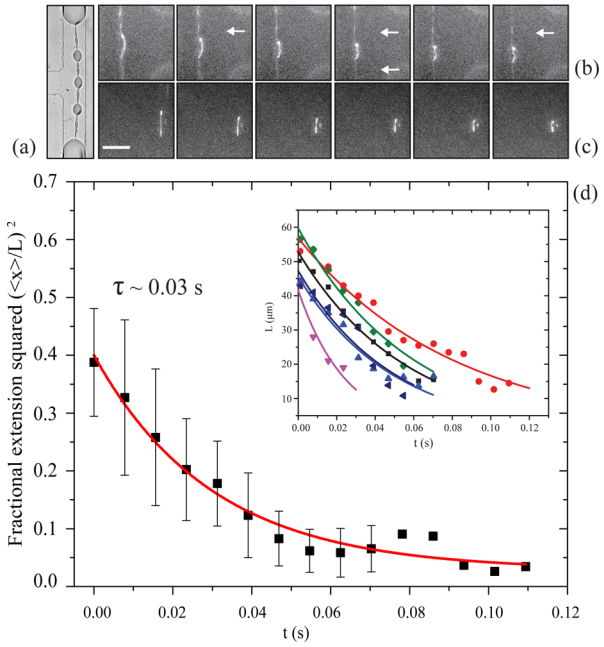

Figure 6. (a) Bright field image of beads-on-a-string morphology in PAA solution. Sequence of fluorescence images showing how single molecules behave during formation of beads on a string morphology in the solution of PAA in (b) Milli-Q water and (c) 25% glycerol. Single polymers gradually recoil inside a bead, and polymeric chains between beads remained stretched (highlighted by white arrows) during this process (the snapshots are after an interval of 15 ms). Scale bar is 50 μm. (d) Time evolution of recoiling-process in the solution of PAA in 25% glycerol. The symbols are average experimental data and represent the time evolution of the square of the fractional extension of six individual DNA molecules relaxing during the beads-on-a-string process. Error bars represent the standard deviation calculated from a set of six measurements. The solid line represents an exponential fit of the form $((\langle x\rangle/L)^2 = C_1 \exp(-t/\tau) + C_2$, where C_1 and C_2 are fitting parameters and the $\langle\ \rangle$ represent an average over six DNA molecules). The characteristic relaxation time (τ) obtained from the fitting is 0.03 s. The inset shows the DNA length versus time, suggesting that the recoiling process occurs for six individual DNA molecules during beads-on-a-string formation.

The microfluidic T-junction also provides an opportunity to investigate the beads-on-a-string morphology at the molecular level. During the last stages of the breakup, the DNA molecules are found to be coiled in the beads, while they are stretched in the strings connecting the beads (see Figure 6b,c). These observations suggest a molecular mechanism in which the fully stretched DNA/polymer molecules coil back to form the beads-on-a-string morphology. Figure 6d displays the time evolution of recoiling process inside a bead for the PAA solution in 25% glycerol−Milli-Q (v/v). The characteristic relaxation time ($\tau \approx$ 0.03 s) of this process is extracted by exponential fitting of square of fractional extension against time.[27,50] The character-

DOI: 10.1021/acs.macromol.6b01755
Macromolecules 2016, 49, 9578−9585

istic relaxation time obtained in Figure 6d is very close to the effective relaxation time estimated from thinning dynamics of PAA solution ($\tau_{eff} \approx 0.06$ s). The estimated relaxation time from shear rheology and Carreau−Yasuda fitting is $\tau_{CY} \approx 53$ s, which is significantly slower than our observed relaxation time based on thinning dynamics and single molecule observation during beads formation process. Recently, Sousa et al.[43] used CaBER rheometer to extract the relaxation time of PAA solutions for investigation of polymeric fluid flow in microscale cross-slot devices. They found that CaBER relaxation time (τ_{Ca}) is also significantly faster than a relaxation time determined from a shear flow (τ_{CY}). Note that the process of polymer/DNA molecules coiling back into the beads of the beads-on-a-string morphology is not a pure relaxation process, and it is possible that it is influenced by fluid flow from the strings into the beads.

CONCLUSION

In conclusion, we have investigated and described the conformation of polymer molecules during thinning and necking of polymeric droplets in an extensional flow provided by a T-shaped microfluidic device. In contrast to the breakup of Newtonian droplets, a stable neck is formed between the separating ends of polymeric droplet that thins down slowly in time. The rate of thinning of the neck is exponential in time, suggesting that the primary flow occurring during the breakup of the droplet is extensional. The overall distribution of molecular extensions in the neck is obtained for the established extensional rate using DNA imaging. This distribution is heterogeneous, indicating that in the neck individual DNA molecules unravel and evolve with different rates and have different steady state extensions. The stretched molecules provide the elastic stresses which stabilize the neck formation during thinning. Moreover, the stretched macromolecules coil back to their equilibrium conformation during the formation of the beads-on-a-string morphology. The present work is only the first step toward understanding a realistic molecular picture for macromolecular solutions under strong extensional flow. We believe that our developed T-shaped microfluidics combined with single molecule experiments can provide a unique opportunity to study the dynamics of single chains in extensional flow fields of polymer solutions (ranging from dilute to well-entangled solutions) with different architectures (from linear to branched polymers).[55,56] These single molecule experiments are required for developing a realistic theoretical picture of polymer solutions in extensional flow fields.

ASSOCIATED CONTENT

Supporting Information

The Supporting Information is available free of charge on the ACS Publications website at DOI: 10.1021/acs.macromol.6b01755.

Additional methods, Figures S1−S6 (PDF)
Movie S1 (AVI)
Movie S2 (AVI)
Movie S3 (AVI)

AUTHOR INFORMATION

Corresponding Author

*E-mail: p.e.boukany@tudelft.nl (P.E.B.).

ORCID

Pouyan E. Boukany: 0000-0002-2262-5795

Notes

The authors declare no competing financial interest.

ACKNOWLEDGMENTS

We acknowledge financial support from European Research Council (ERC) under the European Union's Seventh Framework Programme (FP/2007-2013)/ERC Grant, Agreement No. 337820 (to P.E.B.). We thank Volkert van Steijn and Durgesh Kawale for valuable discussions and help with microfluidic experiments.

REFERENCES

(1) Strutt, J. W.; Rayleigh, L. On the instability of jets. *Proc. London Math. Soc.* **1878**, *10*, 361.
(2) Goldin, M.; Yerushalmi, J.; Pfeffer, R.; Shinnar, R. Breakup of a laminar capillary jet of a viscoelastic fluid. *J. Fluid Mech.* **1969**, *38*, 689−711.
(3) Bousfield, D.; Keunings, R.; Marrucci, G.; Denn, M. Nonlinear analysis of the surface tension driven breakup of viscoelastic filaments. *J. Non-Newtonian Fluid Mech.* **1986**, *21*, 79−97.
(4) Jones, W.; Hudson, N.; Ferguson, J. The extensional properties of M1 obtained from the stretching of a filament by a falling pendant drop. *J. Non-Newtonian Fluid Mech.* **1990**, *35*, 263−276.
(5) Amarouchene, Y.; Bonn, D.; Meunier, J.; Kellay, H. Inhibition of the finite-time singularity during droplet fission of a polymeric fluid. *Phys. Rev. Lett.* **2001**, *86*, 3558.
(6) Mckinley, G. H. Visco-elasto-capillary thinning and break-up of complex fluids. *In Rheology Reviews; British Society of Rheology: Aberystwyth* **2005**, 1−49.
(7) Galindo-Rosales, F. J.; Alves, M.; Oliveira, M. Microdevices for extensional rheometry of low viscosity elastic liquids: a review. *Microfluid. Nanofluid.* **2013**, *14*, 1−19.
(8) Rems, L.; Kawale, D.; Lee, L. J.; Boukany, P. E. Flow of DNA in micro/nanofluidics: From fundamentals to applications. *Biomicrofluidics* **2016**, *10*, 043403.
(9) Glazer, P. J.; Bergen, L.; Jennings, L.; Houtepen, A. J.; Mendes, E.; Boukany, P. E. Generating Aligned Micellar Nanowire Arrays by Dewetting of Micropatterned Surfaces. *Small* **2014**, *10*, 1729−1734.
(10) Matta, J.; Tytus, R. Liquid stretching using a falling cylinder. *J. Non-Newtonian Fluid Mech.* **1990**, *35*, 215−229.
(11) Bazilevsky, A.; Entov, V.; Rozhkov, A. Liquid filament microrheometer and some of its applications. Third European Rheology Conference and Golden Jubilee Meeting of the British Society of Rheology, 1990; pp 41−43.
(12) McKinley, G. H.; Sridhar, T. Filament-stretching rheometry of complex fluids. *Annu. Rev. Fluid Mech.* **2002**, *34*, 375−415.
(13) McKinley, G. H.; Tripathi, A. How to extract the Newtonian viscosity from capillary breakup measurements in a filament rheometer. *J. Rheol. (Melville, NY, U. S.)* **2000**, *44*, 653−670.
(14) Bird, R. B.; Armstrong, R. C.; Hassager, O. *Dynamics of Polymeric Liquids*; John Wiley and Sons Inc.: New York, 1987; Vol. *1*.
(15) Liu, G.; Sun, H.; Rangou, S.; Ntetsikas, K.; Avgeropoulos, A.; Wang, S.-Q. Studying the origin of "strain hardening": Basic difference between extension and shear. *J. Rheol. (Melville, NY, U. S.)* **2013**, *57*, 89−104.
(16) De Gennes, P. Coil-stretch transition of dilute flexible polymers under ultrahigh velocity gradients. *J. Chem. Phys.* **1974**, *60*, 5030−5042.
(17) Anna, S. L.; McKinley, G. H. Elasto-capillary thinning and breakup of model elastic liquids. *J. Rheol. (Melville, NY, U. S.)* **2001**, *45*, 115−138.
(18) Entov, V.; Hinch, E. Effect of a spectrum of relaxation times on the capillary thinning of a filament of elastic liquid. *J. Non-Newtonian Fluid Mech.* **1997**, *72*, 31−53.
(19) Mai, D. J.; Brockman, C.; Schroeder, C. M. Microfluidic systems for single DNA dynamics. *Soft Matter* **2012**, *8*, 10560−10572.
(20) Smith, D. E.; Chu, S. Response of flexible polymers to a sudden elongational flow. *Science* **1998**, *281*, 1335−1340.

DOI: 10.1021/acs.macromol.6b01755
Macromolecules 2016, 49, 9578−9585

(21) Babcock, H. P.; Teixeira, R. E.; Hur, J. S.; Shaqfeh, E. S. G.; Chu, S. Visualization of Molecular Fluctuations near the Critical Point of the Coil-Stretch Transition in Polymer Elongation. *Macromolecules* **2003**, *36*, 4544−4548.
(22) Schroeder, C. M.; Babcock, H. P.; Shaqfeh, E. S.; Chu, S. Observation of polymer conformation hysteresis in extensional flow. *Science* **2003**, *301*, 1515−1519.
(23) Li, Y.; Hsiao, K.-W.; Brockman, C. A.; Yates, D. Y.; Robertson-Anderson, R. M.; Kornfield, J. A.; San Francisco, M. J.; Schroeder, C. M.; McKenna, G. B. When Ends Meet: Circular DNA Stretches Differently in Elongational Flows. *Macromolecules* **2015**, *48*, 5997−6001.
(24) Teixeira, R. E.; Babcock, H. P.; Shaqfeh, E. S. G.; Chu, S. Shear Thinning and Tumbling Dynamics of Single Polymers in the Flow-Gradient Plane. *Macromolecules* **2005**, *38*, 581−592.
(25) Teixeira, R. E.; Dambal, A. K.; Richter, D. H.; Shaqfeh, E. S. G.; Chu, S. The Individualistic Dynamics of Entangled DNA in Solution. *Macromolecules* **2007**, *40*, 2461−2476.
(26) Boukany, P. E.; Hemminger, O.; Wang, S.-Q.; Lee, L. J. Molecular Imaging of Slip in Entangled DNA Solution. *Phys. Rev. Lett.* **2010**, *105*, 027802.
(27) Perkins, T. T.; Smith, D. E.; Chu, S. Single polymer dynamics in an elongational flow. *Science* **1997**, *276*, 2016−2021.
(28) Haward, S. Microfluidic extensional rheometry using stagnation point flow. *Biomicrofluidics* **2016**, *10*, 043401.
(29) Husny, J.; Cooper-White, J. J. The effect of elasticity on drop creation in T-shaped microchannels. *J. Non-Newtonian Fluid Mech.* **2006**, *137*, 121−136.
(30) Steinhaus, B.; Shen, A. Q.; Sureshkumar, R. Dynamics of viscoelastic fluid filaments in microfluidic devices. *Phys. Fluids* **2007**, *19*, 073103.
(31) Arratia, P. E.; Gollub, J. P.; Durian, D. J. Polymeric filament thinning and breakup in microchannels. *Phys. Rev. E* **2008**, *77*, 036309.
(32) Arratia, P. E.; Cramer, L.; Gollub, J. P.; Durian, D. J. The effects of polymer molecular weight on filament thinning and drop breakup in microchannels. *New J. Phys.* **2009**, *11*, 115006.
(33) Christopher, G.; Anna, S. Passive breakup of viscoelastic droplets and filament self-thinning at a microfluidic T-junction. *J. Rheol. (Melville, NY, U. S.)* **2009**, *53*, 663−683.
(34) Lee, W.; Walker, L. M.; Anna, S. L. Competition between viscoelasticity and surfactant dynamics in flow focusing microfluidics. *Macromol. Mater. Eng.* **2011**, *296*, 203−213.
(35) Juarez, G.; Arratia, P. E. Extensional rheology of DNA suspensions in microfluidic devices. *Soft Matter* **2011**, *7*, 9444−9452.
(36) Ingremeau, F.; Kellay, H. Stretching polymers in droplet-pinch-off experiments. *Phys. Rev. X* **2013**, *3*, 041002.
(37) Hu, X.; Boukany, P. E.; Hemminger, O. L.; Lee, L. J. The Use of Microfluidics in Rheology. *Macromol. Mater. Eng.* **2011**, *296*, 308−320.
(38) Duffy, D. C.; McDonald, J. C.; Schueller, O. J.; Whitesides, G. M. Rapid prototyping of microfluidic systems in poly (dimethylsiloxane). *Anal. Chem.* **1998**, *70*, 4974−4984.
(39) Xia, Y.; Whitesides, G. M. Soft lithography. *Annu. Rev. Mater. Sci.* **1998**, *28*, 153−184.
(40) Francois, J.; Sarazin, D.; Schwartz, T.; Weill, G. Polyacrylamide in water: molecular weight dependence of < R2> and [η] and the problem of the excluded volume exponent. *Polymer* **1979**, *20*, 969−975.
(41) Doi, M.; Edwards, S. F. *The Theory of Polymer Dynamics*; Oxford University Press: 1988; Vol. *73*.
(42) Campo-Deaño, L.; Galindo-Rosales, F. J.; Pinho, F. T.; Alves, M. A.; Oliveira, M. S. Flow of low viscosity Boger fluids through a microfluidic hyperbolic contraction. *J. Non-Newtonian Fluid Mech.* **2011**, *166*, 1286−1296.
(43) Sousa, P. C.; Pinho, F. T.; Oliveira, M. S. N.; Alves, M. A. Purely elastic flow instabilities in microscale cross-slot devices. *Soft Matter* **2015**, *11*, 8856−8862.
(44) Reed, W. F.; Ghosh, S.; Medjahdi, G.; Francois, J. Dependence of polyelectrolyte apparent persistence lengths, viscosity, and diffusion on ionic strength and linear charge density. *Macromolecules* **1991**, *24*, 6189−6198.
(45) Ait-Kadi, A.; Carreau, P.; Chauveteau, G. Rheological properties of partially hydrolyzed polyacrylamide solutions. *J. Rheol. (Melville, NY, U. S.)* **1987**, *31*, 537−561.
(46) Magueur, A.; Moan, G. M.; Chauveteau, G. Effect of Successive Contractions and Expansions on the Apparent Viscosity of Dilute Polymer Solutions. *Chem. Eng. Commun.* **1985**, *36*, 351−366.
(47) Rubinstein, M.; Colby, R. H. *Polymer Physics*; Oxford University: New York, 2003.
(48) Eggers, J. Nonlinear dynamics and breakup of free-surface flows. *Rev. Mod. Phys.* **1997**, *69*, 865.
(49) Tirtaatmadja, V.; Sridhar, T. A filament stretching device for measurement of extensional viscosity. *J. Rheol. (Melville, NY, U. S.)* **1993**, *37*, 1081−1102.
(50) Liu, Y.; Jun, Y.; Steinberg, V. Concentration dependence of the longest relaxation times of dilute and semi-dilute polymer solutions. *J. Rheol. (Melville, NY, U. S.)* **2009**, *53*, 1069−1085.
(51) Gerashchenko, S.; Chevallard, C.; Steinberg, V. Single-polymer dynamics: Coil-stretch transition in a random flow. *EPL (Europhysics Letters)* **2005**, *71*, 221.
(52) François, N.; Lasne, D.; Amarouchene, Y.; Lounis, B.; Kellay, H. Drag enhancement with polymers. *Phys. Rev. Lett.* **2008**, *100*, 018302.
(53) François, N.; Amarouchene, Y.; Lounis, B.; Kellay, H. Polymer conformations and hysteretic stresses in nonstationary flows of polymer solutions. *EPL (Europhysics Letters)* **2009**, *86*, 34002.
(54) Smith, M.; Bertola, V. Effect of polymer additives on the wetting of impacting droplets. *Phys. Rev. Lett.* **2010**, *104*, 154502.
(55) Mai, D. J.; Marciel, A. B.; Sing, C. E.; Schroeder, C. M. Topology-Controlled Relaxation Dynamics of Single Branched Polymers. *ACS Macro Lett.* **2015**, *4*, 446−452.
(56) Dinic, J.; Zhang, Y.; Jimenez, L. N.; Sharma, V. Extensional Relaxation Times of Dilute, Aqueous Polymer Solutions. *ACS Macro Lett.* **2015**, *4*, 804−808.

DOI: 10.1021/acs.macromol.6b01755
Macromolecules 2016, 49, 9578−9585